Preprints (www.preprints.org) | NOT PEER-REVIEWED | Posted: 4 October 2017 doi:10.20944/preprints201710.0027.v1

Review

Advances in concentrating solar power tower

Albert Boretti [1,*], Stefania Castelletto [2] and Sarim Al-Zubaidy [3]

[1] Department of Mechanical and Aerospace Engineering (MAE), Benjamin M. Statler College of Engineering and Mineral Resources, West Virginia University, Morgantown, WV 26506, United States, alboretti@mail.wvu.edu; alboretti@mail.wvu.edu ; a.a.boretti@gmail.com

[2] School of Engineering, RMIT University, Bundoora, VIC 3083, Australia; stefania.castelletto@gmail.com

[3] The University of Trinidad and Tobago, Trinidad and Tobago; president@utt.edu.tt

* Correspondence: alboretti@mail.wvu.edu ; a.a.boretti@gmail.com

Abstract: The paper examines design and operating data of current concentrated solar power (CSP) solar tower (ST) plants. The study includes CSP with or without boost by combustion of natural gas (NG) and with or without thermal energy storage (TES). The study then reviews the novel trends to produce better ratio of solar field power to electric power, better capacity factor, better matching of production and demand, lower plant's cost and increased life span of plant's components. The key areas of progress of CSP ST technology briefly summarized are materials and manufacturing processes, design of solar field and receiver, receiver and power block fluids, power cycle parameters, optimal management of daily and seasonal operation of the plant, new thermal energy storage concepts, integration of solar plant with thermal desalination, integration of solar plant with combined cycle gas turbine (CCGT) installations and finally, specialization and regionalization of the project specification.

Keywords: renewable energy, concentrated solar power, solar tower, parabolic trough, natural gas boost, thermal energy storage, molten salt, steam, Rankine cycles

---

1. Introduction

The basic principles of concentrated solar power (CSP) systems are covered in reference works such as [1]. Lenses or mirrors concentrate the sun light energy on a small area. The concentrated light is then converted to heat at high temperature. The heat is finally transferred to a power cycle working fluid (typically water/steam). Superheated steam typically drives a Rankine steam turbine cycle. Concentrators differ in the way they track the sun and focus the light. The most popular concentrating technologies are Parabolic Trough (PT) and Solar Tower (ST). Different concentrators provide different receiver temperature and peak temperature of the steam for the power cycle, with correspondingly varying thermal efficiency of the power cycle. In addition to the type of receiver and the solar field feeding this receiver, also the receiver fluid (RF) plays a role in the peak temperatures of the steam. Current RFs include oil, molten salt (MS) or water/steam. Intermediate heat exchangers are needed between oil or MS and water/steam. MS permits thermal energy storage (TES) in hot and cold reservoir to decouple electricity production from availability of sun light. While an additional MS circuit has been proposed as an appendage to existing CSP plants with oil as RF, MS provides better outcome when used directly as the RF. Replacement of oil with MS permits operation at higher temperatures for higher steam temperature and efficiency of power generation. Additionally, it lowers the cost of TES. Direct use of water/steam as a RF has the advantage of simplicity, cost and sometimes efficiency. However, this links the production of electricity to sun availability. Condensation of steam usually occurs in air-cooled towers. Water cooled condensers may permit better power cycle efficiencies but are impractical in mostly desert locations.

Preprints (www.preprints.org) | NOT PEER-REVIEWED | Posted: 4 October 2017 doi:10.20944/preprints201710.0027.v1

By using the combustion of natural gas (NG), it is possible to drastically improve the match between production and demand of CSP plants. However, boost by NG is reasonable only if performed in minimal extent, for both efficiency of energy use and regulations concerning emissions of carbon dioxide.

The use of NG in a combined cycle gas turbine (CCGT) plant occurs with a fuel conversion efficiency that is about double the efficiency of a CSP plant operated with NG only (η above 60% vs. η around 30%). The spreading in between the η of a CSP plant and a NG fueled plant is similarly large in cases of cogeneration, where the gas turbine (GT) plant also features production of process heat, for heating, cooling, desalination or other activities. Therefore, it is not efficient to design a CSP ST plant requiring a significant NG combustion.

The global market of CSP is dominated by PT plants, about 90% of all the CSP plants, regardless the world largest CSP plant (Ivanpah Solar Electric Generating System, ISEGS) uses ST technology. ISEGS is made up of three installations one close to the other. The second largest CSP project in the world, the Solar Energy Generating Systems (SEGS) facility, is based on PT. This project is made of nine different installations.

The ST technology offers theoretically higher efficiency because of higher temperature. However, the technology is also more demanding from economic and technical view-points. ST developments are less advanced than PT systems.

The net capacity of ISEGS is 377 MW, while the net capacity of SEGS II-IX is 340 MW. Both facilities use NG to boost the electricity production. ISEGS uses NG in a greater extent than the SEGS facilities. Both ISEGS and SEGS lack of TES. The actual capacity factors (ε) of both installations (electricity produced in a year divided by the product of net capacity by number of hours in a year) is about 20% neglecting the boost by combustion of NG everything but negligible.

The CSP technologies presently do not compete on price with photovoltaics (PV) solar panels that have progressed massively in recent years because of the decreasing prices of the PV panels and the much smaller operating costs.

While the total solar electricity generation (2015) is 253.0 TW·h, or 1.05% of the total, CSP plants represent (2015) less than 2% of the worldwide installed capacity of solar electricity plants, for a total CSP contribution to the global energy mix of about 0.02%. This scenario is expected to drastically change in the next few years, and there is a clear need to develop new CSP ST technologies to match the significant demand.

Ref. [2] discusses the most relevant drivers and barriers for the deployment of concentrated solar power (CSP) in the EU by 2030. Apart from supporting policies, the most relevant drivers are the higher value of CSP compared to other renewable energy technologies, and the substantial cost reductions that are expected for the technology. The most relevant barriers are the still very high cost of the technology when compared to conventional power plants and other renewable energy technologies, and the uncertain about policies. Hence, costs of the CSP technology is the key factor for a growth. Similarly, Ref. [3] discusses the main reasons why Chinese and Brazilian energy policies so far have not been focused on CSP. As the high Levelized Cost of Electricity (LCOE) of large scale deployment of CSP technologies may affect the competitiveness of national industry in global markets, a comprehensive answer may only follow global policies. CSP has not benefited so far from the global demand that has boosted wind and solar photovoltaic with their subsequent price reductions.

Preprints (www.preprints.org) | NOT PEER-REVIEWED | Posted: 4 October 2017 doi:10.20944/preprints201710.0027.v1

2. Current solar tower and parabolic trough installations

2.1 Parabolic trough

The most common CSP systems are PT. A PT is made up of a linear parabolic reflector concentrating the sun light onto a tubular receiver. The receiver is located along the focal line of the reflector. The tubular receiver is filled with a working fluid. The RF may be oil, MS or water/steam. The reflectors follow the sun with tracking along a single axis. The working fluid is heated as it flows through the receiver up to temperatures from 390 to 500 °C, depending on the fluid used. If oil or MS, this fluid is then used as the heat driving the production of steam for the power cycle in a heat exchanger. The shaped mirrors of a PT focus the sun light on a tube running along the focus line with an 80x concentration. The sun light is absorbed by tube that is often in a glass vacuum, and delivered to the RF. PT are less efficient than ST. They are however much simpler and they are less expensive to build and operate. Hence, the much wider use.

Reference PT specifications change with the RF and the availability of TES (data from [4], [5], [6], [7], [8]). For oil as the RF, the receiver temperature is 390 ºC, the peak flux on receiver is 25 W/m^2, the hot storage temperature is 390 ºC, the cold storage temperature is 290 ºC, and the condenser temperature for heat rejection is 40 ºC. For MS (nitrate salt) as the RF, the receiver temperature is 500 ºC, the peak flux on receiver is 25 kW/m^2, the hot storage temperature is 500 ºC, and the cold storage temperature is 300 ºC. In case of water/steam as the RF, the receiver temperature is 500 ºC, the peak flux on receiver is 25 kW/m^2. The hot and cold storage tanks are not available in this case.

2.2 Solar tower

A ST concentrates the sun light from a field of heliostats on a central tower. The heliostats are dual axis tracking reflectors grouped in arrays. They concentrate sunlight on a relatively small central receiver located at the top of the tower. The sun light with ST is much more concentrated than in PT. The RF may be heated to temperatures from 500 to 1000 °C depending on the RFs and the solar concentration design. When MS is used, it serves as the heat driving the production of steam for the power cycle in a heat exchanger. When water/steam is used, then there is no need of this heat exchanger.

The field of heliostats focus the light on top of the tower with a 500x to 1000x concentration. Light is absorbed by metal tubes and delivered to the RF, either water/steam or MS (nitrate salt). Due to sunlight shaded, blocked, absorbed, or spilled, there is a 40% loss of incident light collected by the RF. Receiver, piping, and tank thermal losses further reduced the amount of energy transferred to the power cycle.

The reference ST specifications change with the RF and the availability of TES (data from [4], [8], [9], [10]). For MS (nitrate salt) as the RF, the receiver temperature is 565 ºC, the peak flux on receiver is 1,000 kW/m^2, the hot storage temperature is 565 ºC, the cold storage temperature is 290 ºC, and the condenser temperature for heat rejection is 40 ºC. In case of water/steam as the RF, the receiver temperature is 550 ºC, the peak flux on receiver is > 300 kW/m^2. The hot and cold storage tanks are not available in this case.

2.3 Rice facility

A scheme of the Rice concentrating ST facility is provided in figure 1 (from [11]). The Rice Solar Energy Project was a latest generation CSP ST project [12] put on hold. The proposed location was

Preprints (www.preprints.org) | NOT PEER-REVIEWED | Posted: 4 October 2017 doi:10.20944/preprints201710.0027.v1

Rice, California (Mojave Desert, near Blythe). The gross turbine capacity is 150 MW. The land area is 5.706 km². The solar resource is 2,598 kWh/m²/year.

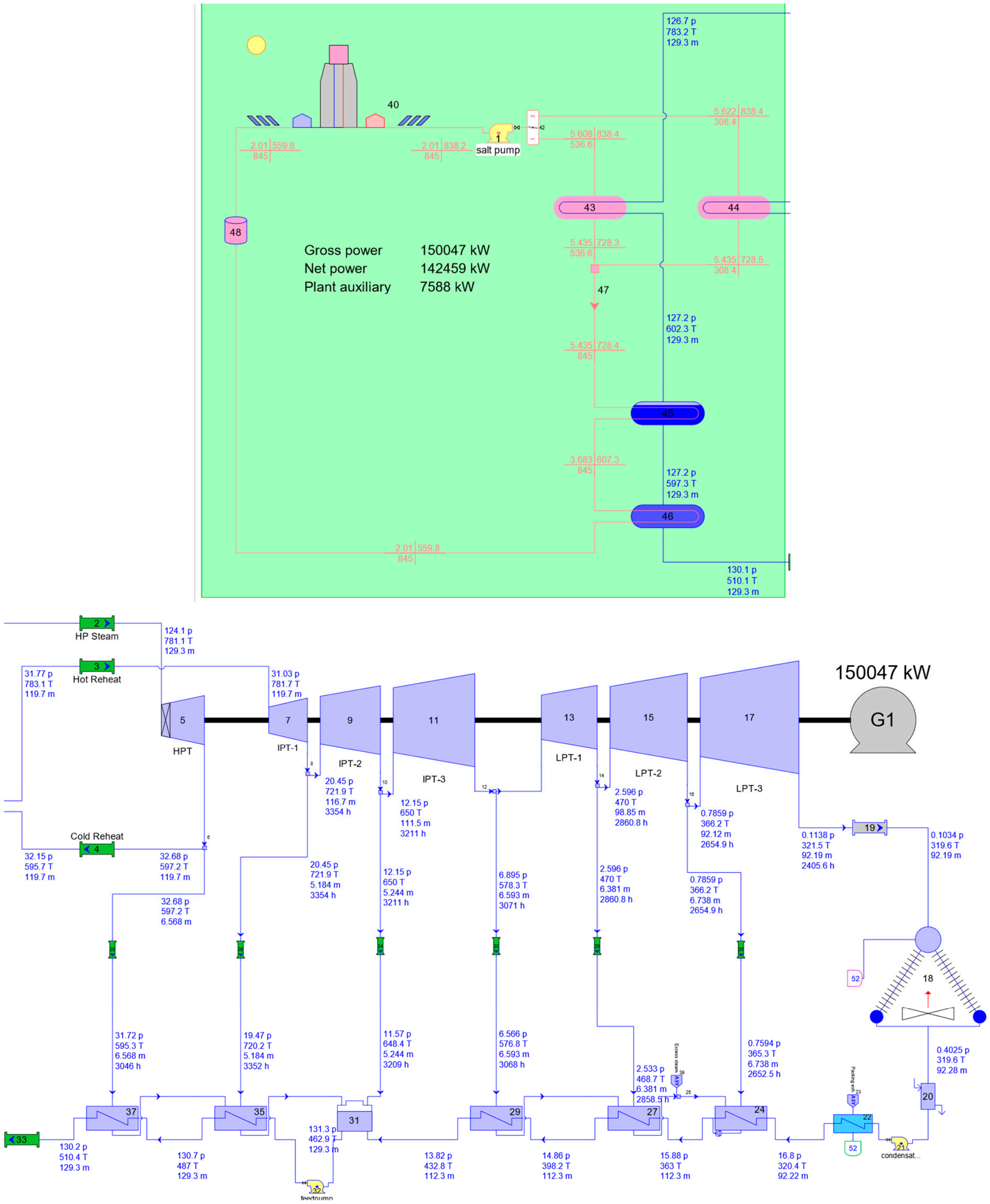

Figure 1 – Thermoflow scheme of the design point balance for the Rice concentrating ST facility. Courtesy of Thermoflow, www.thermoflow.com. All data extracted from public available sources, California Energy Commission.

Planned electricity generation was 450,000 MWh/year. The heliostat solar-field aperture area is 1,071,361 m². The number of heliostats is 17,170, and every heliostat has an aperture area of 62.4 m². The tower height is 164.6 m. The receiver type is external, cylindrical. The heat-transfer fluid is MS. The receiver inlet temperature is 282 °C, and the receiver outlet temperature is 566 °C. The steam

Preprints (www.preprints.org) | NOT PEER-REVIEWED | Posted: 4 October 2017 doi:10.20944/preprints201710.0027.v1

Rankine power cycle has a maximum pressure of 115 bar. The cooling method is dry cooling. The TES is achieved by raising MS temperature from 282 °C to 566 °C. The TES efficiency is 99%.

2.4 Operational data of ISEGS, SEGS and Solana

Plant level data of electricity production and NG consumption of CSP plants in the United States are provided in [13]. Data of [13] includes the energy input from both the sun and the natural gas. Capacity factors of CPS plants with and without NG boost have been discussed and compared in [8]. The capacity factor ε_1 is defined as the ratio of the actual electricity produced in a year E [MW·h] vs. the product of net capacity P [MW] by number of hours in a year (8760):

$$\varepsilon_1 = \frac{E}{P \cdot 8760} \quad (1)$$

This capacity factor does not account for the consumption of NG.

Ref. [8] suggests as a first opportunity to account for the NG consumption by multiplying the above capacity factor by the ratio of the solar energy input Q_{Sun} to the total solar energy and NG energy input $Q_{Sun}+Q_{NG}$, all in [MW·h]:

$$\varepsilon_2 = \frac{E}{P \cdot 8760} \cdot \frac{Q_{Sun}}{Q_{Sun} + Q_{NG}} \quad (2)$$

Ref. [8] suggests two other capacity factors.

A third capacity factor ε_3 is defined as the ratio of the actual electricity produced reduced of the electricity produced by burning the NG in a GT plant of η_{GT}=30%, vs. the product of net capacity by number of hours in a year:

$$\varepsilon_3 = \frac{E - Q_{NG} \cdot \eta_{GT}}{P \cdot 8760} \quad (3)$$

A fourth capacity factor ε_4 is finally defined as the ratio of the actual electricity produced reduced of the electricity produced by burning the NG in a CCGT plant of η_{CCGT}=60%, vs. the product of net capacity by number of hours in a year:

$$\varepsilon_4 = \frac{E - Q_{NG} \cdot \eta_{CCGT}}{P \cdot 8760} \quad (4)$$

An important parameter not accounted for in this assessment is the electricity generation profile requested from a specific facility. The largest is the departure of the electricity generation profile from the sun energy profile during a day, the more difficult is to achieve a large capacity factor. Also, not considered in this assessment, is the maximum electric power produced vs. the summer solstice peak sun power collected by the heliostats that may strongly vary across the projects.

The capacity factors of the three largest CSP projects, ISEGS (ST, no TES, NG boost), SEGS (PT, no TES, NG boost) and Solana (PT, TES, no NG boost), are given in Ref. [8].

Over the period July 2016 to June 2017, without accounting for the NG consumption, ε_1 were 22.98%, 21.59% and 23.67% for ISEGS 1-2-3, 22.54% for SEGS IX and 32.65% for Solana.

By accounting for the consumption of the NG at the actual energy conversion efficiency η of the plant, ε_2 are smaller for ISEGS 1-2-3 at 19.20%, 18.04% and 20.12% and smaller for SEGS IX at 19.91%, while obviously $\varepsilon_2=\varepsilon_1$ for Solana.

By considering the energy conversion efficiency of a reference GT plant η=30%, the ε_3 are marginally better in ISEGS 1-2-3 and SEGS IX while $\varepsilon_3=\varepsilon_1$ for Solana.

Preprints (www.preprints.org) | NOT PEER-REVIEWED | Posted: 4 October 2017 doi:10.20944/preprints201710.0027.v1

Finally, by accounting for the consumption of the NG at the energy conversion efficiency of a reference CCGT plant η=60%, ε_4 are much smaller for ISEGS 1-2-3 at 15.83%, 14.80% and 17.07%, and much smaller for SEGS IX at 17.91%, while $\varepsilon_4=\varepsilon_1$ for Solana.

This analysis demonstrates that TES plays a significant role in producing much higher capacity factors in present installations, and the use of NG to boost the electricity production in a CSP plant is illogic, being the fuel energy used at a much lower efficiency than in a CCGT plant.

The approximate cost of the 377 MW ISEGS ST project is about 2,200 USD million (2014 values), corresponding to about 2,272 USD million in August 2017 [8].

As one of the 33 MW SEGS Kramer Junction facilities required 90 USD million to build (1999 values), the approximate cost of a project delivering same net capacity of ISEGS ST on SEGS PT technology would be 1,569 USD million in August 2017 [8].

The cost of Solana (PT, TES) is approximately 2,000 USD million, 10% less than the ISEGS ST facility that was completed only two months later, however for 34% less net capacity [8].

Therefore, present cost of CSP solar energy is everything but economic, while the actual production of electricity is much less than the values claimed by the manufacturers. This translates in an urgent need to further progress current technologies as well as to develop new technologies.

3. Review of development trends in solar tower technology

Design, construction and operating technical and economic issues are considered in the literature to various extents. CSP ST have many variants for receivers, working fluids, power cycles, type, number and layout of heliostats, height of tower, condenser, turbine, heat exchangers and thermal energy storage. Since most part of the existing plants are demonstration plants, the full potential of the ST technology is not shown by surveys of plants.

As an example of a preliminary introductory survey, Ref. [14] examines some of the main parameters of existing plants, solar energy to electricity conversion efficiency, and mirror and land area per MW_e of capacity, packing density, configuration of the field layout, receiver size, tower height and cost of the plant. The annual solar energy to electricity conversion efficiency corresponds to an average of about 16%. The packing density has an average of about 20%.

Similarly, paragraph 2.4 above proposed (from [8]) the energy outputs and costs of ISEGS (ST), SEGS (PT) and Solana (PT, MS TES). ISEGS is the state-of-the-art of the operational CSP ST technology.

Development trends are proposed here after.

3.1 Receiver and thermal energy storage fluids

TES is the key to achieve high capacity factors and avoid NG boost. TES allows improved dispatch-ability (generation on demand) of power from a CSP plant. TES drastically increases the annual capacity factor. The MS TES technology is the best avenue to generate non-intermittent electricity with CSP and achieve capacity factors above 0.3, and potentially up to 0.4. A 10 hour TES eliminates the need for a NG back up or boost of electricity production at sunrise and in the evening peak hours [8].

Next generation CSP plants will very likely consist of four major units, solar field to concentrate the sun light energy, ST MS receiver to convert the solar energy into thermal energy, TES section to store the thermal energy using the MS, and finally power block generating electricity through a

Preprints (www.preprints.org) | NOT PEER-REVIEWED | Posted: 4 October 2017 doi:10.20944/preprints201710.0027.v1

steam turbine. While the cost will further increase because of the TES, it will be paid back by the increased production and dispatch-ability.

The current best RF and TES fluid is MS that, however, has the drawback of having low degradation temperature and high melting temperature, in addition to other downfalls such as corrosion and heat tracing. Solar salt, 60% $NaNO_3$ and 40% KNO_3, is used as a low-cost RF and TES fluid. MS temperatures typically go up to 565 °C. This permits superheated steam generation. MS has good heat transfer characteristics [15]. As major downfalls, the salt is freezing below 220 °C, heat tracing is required, and draining of receiver and other system components during the night must be provided. Furthermore, the salt may degrade at temperatures higher than 600 °C and depending on salt quality it can generate corrosion of metallic components [15].

Alternative fluids are therefore under investigation for a broader range of operation and for cost and performance advantages, as RF and / or the TES fluid. The power block fluid is usually water/steam, but other fluids are also considered for the power block, as it is discussed in another paragraph. There is obviously the opportunity to use a single fluid as receiver, TES and power block fluid. Water/steam is the most obvious example.

Ref. [16] reviewed various types of RF including air, water/steam, thermal oils, organic fluids, molten-salts and liquid metals. The different alternatives were compared with reference melting temperature, thermal stability and corrosion with stainless steels and nickel based alloys the piping and container materials. MS show advantages operating up to 800 °C.

Different alternatives for the RF are mentioned in ref. [15]. The presentation includes alternative RF as well as receiver technologies. MS, water/steam, air in open/closed systems, liquid metals, solid particles and other gases are considered as heat transfer medium. Classification is by maturity of technologies. It includes MS and water/steam as state of the art technology, open volumetric air receiver as “first-of-its-kind” technology, then pressurized air receivers as technology in pilot phase, liquid metals and solid particles as technology under development. The different receiver technologies proposed in [15] are reviewed in a subsequent specific paragraph.

Ref. [17] studies the impact of the fluid in a flat plate, high temperature, TES unit with flat slabs of phase change materials. Six gaseous and liquid fluids are compared. For the capacity rate considered, liquid sodium was the best performing (99.4% of the ideal electricity to grid). Solar salt achieved a 93.6% performance. Atmospheric air, air at 10 bars, s-CO_2 at 100 bar and steam at 10 bar achieved performances between 87.9% and 91.3%. The work concludes that gases are comparable to liquids as TES fluids for the specific application and it mentions that gases may also be used as the working fluid in the power block.

Ref. [18] reviews the CSP TES systems. Various aspects are discussed including trend of development, different technologies of TES systems for high temperature applications (200–1000°C) with a focus on thermochemical heat storage, and storage concepts for their integration in CSP plants. TES systems are considered a necessary option for more than 70% of the new CSP plants being developed. Sensible heat storage technology is the most used TES in CSP plants in operation, for their reliability, low cost, easy to implementation and large experimental feedback. Latent and thermochemical energy storage (TCES) technologies have much higher energy density. This gives them better perspectives for future developments. TCES are specifically covered in a following paragraph. New concepts for TES integration include coupled technology for higher operating temperature and cascade TES of modularized storage units for intelligent temperature control.

Preprints (www.preprints.org) | NOT PEER-REVIEWED | Posted: 4 October 2017 doi:10.20944/preprints201710.0027.v1

Ref. [19] reviews the current commercial TES systems used in CSP plants either steam accumulators or MS. The economic value of the TES system is assessed by the calculation of the LCOE, an economic performance metric, of the TES itself rather than the full plant. Calculations were done for different plant configurations and storage sizes varying from 1 to 9 h of operation at full capacity. LCOE is shown to be a valid argument for the selection of the TES, even if other aspects not included also play a relevant role.

Ref. [20] considers the opportunity to adopt particle suspensions as RF, TES fluid, and power block fluid. Values of the heat transfer coefficient up to 1,100 $W/m^2/K$ (bare tubes) and 2,200 $W/m^2/K$ (finned tubes) were obtained for operation of a pilot plant at low superficial gas velocities of 0.04–0.19 m/s limiting heat losses by the exhaust air. Despite additional costs for particle handling and an appropriate boiler, the required overall investment and operating costs are significantly lower than the reference MS system, leading to a reduction in LCOE from approximately 125 €/MWh to below 100 €/MWh.

Ref. [21] reviews the developments of the last five years and expected for the near future of the most important components of a CSP ST: water/steam, air or CO_2 power cycles; water/steam, MS, liquid metals, particles or chemically reacting fluids and the RF; design of heliostats; design of receivers, volumetric, tubular, solar particle receivers; TES and hybridization. They conclude that there will certainly be an increase number of CSP ST in the near future, but with a significant hold-back until standardization and experience is gained. Within the next 5 years, plants will use either MS or water/steam as the receiver fluid, but most of them will have MS TES. In a 10 years' time, more plants will be MS with TES. The commercial plant designs in 10 years will not differ too much from the commercial plant designs of today.

3.2 Thermochemical energy storage

In addition to the classic TES design with two tanks of a properly selected TES fluid, TCES systems have been also proposed. TCES is the reversible conversion of solar-thermal energy to chemical energy.

Ref. [22] reviews the TCES systems. TCES has high energy density and low heat loss over long periods than the MS TES. CSP plants with TCES systems are modelled, and sample computational results are provided for ammonia and methane systems with two gas storage options. The gas storage is identified as the main cost driver. The compressor electricity consumption is identified as the main energy driver.

Ref. [23] reports of a pilot-scale redox-based TCES system. The storage unit is made of inert honeycomb supports (cordierite) coated with 88 kg of redox active material (cobalt oxide). When crossing respectively the reduction/oxidation temperature of the Co_3O_4/CoO pair, the heat absorbed or released by the chemical reaction allows to store or release energy at constant temperature. Within the limit of a campaign of 22 thermochemical charge/discharge cycles, there was no measurable cycle-to-cycle degradation. The system average capacity was very close to the ideal case. The TCES system offers a storage capacity of 47.0 kW·h vs. the 25.3 kW·h of the same volume of a sensible-only storage unit made of uncoated cordierite honeycombs.

3.3 Design of power cycles and power cycles fluids

Supercritical steam [24] and supercritical CO_2 [25] power cycles are being considered to improve the conversion efficiency thermal-electric cycles.

Preprints (www.preprints.org) | NOT PEER-REVIEWED | Posted: 4 October 2017 doi:10.20944/preprints201710.0027.v1

Ref. [26] computed the thermodynamic irreversibility such as convective and radiative loss on tower receiver and thermal resistance in heat exchangers. Increasing the receiver working temperature increases both thermal and exergy conversion efficiencies only until an optimum temperature is reached. The optimum temperature increases with the concentration ratio. Increasing the concentration ratio, the conversion efficiency increases only until an optimum concentration ratio is reached. Increasing the end reversible engine efficiency increases the thermal conversion efficiency until a maximum value is reached. Then, the conversion efficiency drops dramatically.

The performance of an integrally geared compressor-expander recuperated recompression cycle with sCO_2 as the working fluid is modeled in Ref. [27]. Mostly through reduced power block cost and a better cycle model, the LCOE is computed to be 5.98 ¢/kWh.

Ref. [28] reviews advanced power cycles under consideration for CSP. Supercritical steam turbines are attractive at large scale but presently commercial products are too large for today's CSP ST plants. SCO_2 closed loop Brayton cycles are early in their development but promise high efficiency at reasonable temperatures across a range of capacities. In perspective, these cycles may significantly lower the costs. GT combined cycles driven by CSP are one of the highest efficiency options available. Other bottoming and topping cycle configurations are also considered. High temperature component demonstration is indicated as a critical factor.

Three different sCO_2 power cycles applied to a high temperature ST CSP system are considered in Ref. [29]. Maximum temperatures are up to 800 °C. The fluid to transfer energy from the receiver to the power block is KCl-$MgCl_2$ MS. The highest efficiency at design conditions is achieved by the Recompression with Main Compression Intercooling (RMCI) configuration with a solar energy to electricity efficiency of 24.5% and a maximum temperature of 750 °C. The yearly energy yield is 18.4%. The performance decay from design to average yearly conditions is mostly due to the optical and thermal efficiencies reduction respectively -10.8% and -16.4%.

Ref. [30] reviews several current sCO_2 Brayton cycles for integration into a MS CSP ST system. The intercooling cycle can generally offer the highest efficiency, followed by the partial cooling cycle, and the recompression cycle. The pre-compression cycle can yield higher efficiency than the recompression cycle when the compressor inlet temperature is high. The increase in the hot salt temperature cannot always result in an efficiency improvement. The partial cooling cycle can offer the largest specific work, while the recompression cycle and the split expansion cycle yield the lowest specific work. The MS temperature differences with the simple recuperation cycle, the partial-cooling cycle, and the pre-compression cycle are slightly larger than those with the recompression cycle, the split expansion cycle, and the intercooling cycle. Reheating can decrease the system efficiency in the cases with high hot MS temperature. Larger MS temperature difference may be achieved without reheating than with reheating. While current sCO_2 Brayton cycle offer high efficiency, challenges for integrating them includes the specific work that is relatively small, and the temperature difference across the solar receiver that is narrow.

Ref. [31] studied more efficient Rankine power cycles. The temperature and pressure of the main steam and the reheating pressure affect the temperature of the MS in the receiver. If the temperature increases, the receiver efficiency decreases but the power block efficiency increases. If the pressure at the inlet of the turbine increases, the efficiency of the power block increases even more than by increasing the temperature. The reheating pressure is the most influential factor on the plant efficiency. A high reheating pressure decreases the plant efficiency. The best efficiencies were

Preprints (www.preprints.org) | NOT PEER-REVIEWED | Posted: 4 October 2017 doi:10.20944/preprints201710.0027.v1

obtained for the supercritical cycle with a low reheating pressure and high temperature. The subcritical cycle at high pressure and temperature performed closely. The investment cost of the different cycles increases with the pressure and the temperature of the power block. Subcritical cycles are less expensive than supercritical cycles even if the cost increase is balanced by the efficiency increase. Subcritical cycles working at 16 MPa and supercritical cycles working with low reheating pressure deliver the same cost per MW_e.

Energy and exergy analyses of sCO_2 recompression Brayton cycles are proposed in Ref. [32]. The heliostat field layout is optimized for the optical performance on an annual basis. A recompression Brayton cycle uses the heat collected at the receiver. An auxiliary boiler is added prior to the turbine to keep the turbine inlet temperature constant. The net power output is constant 40 MW. The highest exergy destruction occurs in the heliostat field. The second highest exergy destruction happens in the boiler's combustion chamber. The combustion exergy destruction rate increases during the winter months when the solar radiation decreases.

Ref. [33] studied the thermal performance of an array of pressurized air solar receiver modules integrated to a GT power cycle for a simple Brayton cycle, a recuperated Brayton cycle, and a combined Brayton-Rankine cycle. The solar receiver's solar energy to heat efficiency decreases at higher temperatures and pressures. The opposite is true for the power cycle's heat to work efficiency. The optimal operating conditions are achieved with a preheat stage for a solar receiver outlet air temperature of 1300 °C and an air cycle pressure ratio of 9, yielding a peak solar energy to electricity efficiency of 39.3% for the combined cycle.

Alternative cycles' technology certainly needs more work before introduction in full scale CSP ST plants where water/steam Rankine cycles are the best short term solution.

3.4 Optimized design of solar field and receiver

A classification by maturity of receiver technologies is proposed in [15] and has been included in a prior paragraph. In addition to MS and water/steam state of the art technologies, open volumetric air receiver, pressurized air receivers, liquid metals and solid particles are all technologies being developed at different stages of evolution.

As the receiver design is not decoupled from the design of the solar field, here we couple together these two aspects.

Ref. [34] reviewed gas receivers, liquid receivers, and solid particle receivers. Higher thermal-to-electric efficiencies of 50% and higher may be achieved by using supercritical CO_2 closed-loop Brayton cycles and direct heating of the CO_2 in tubular receiver designs, external or cavity, for high fluid pressures of about 20 MPa and temperatures of about 700 °C. Indirect heating of other fluids/materials that can be stored at high temperatures such as advanced MS, liquid metals, or solid particles are also possible, but with additional challenges such as stability, heat loss, and the need for high-temperature heat exchangers.

As per [15], strategies aimed at improving MS systems include higher temperature MS, higher steam parameters, smaller heat exchanger, smaller storage, less critical receiver temperature operation. Means to improve the receiver efficiency include reduction of thermal losses, cavity arrangement, face down can design, standard vacuum absorber for first temperature step, and selective coatings for higher absorption of solar radiation [15]. Optimization of operation includes real time aim point strategy for homogenous receiver temperature, solar pre-heating of receiver, faster start-up and elimination of draining of receiver during clouds [15].

Preprints (www.preprints.org) | NOT PEER-REVIEWED | Posted: 4 October 2017 doi:10.20944/preprints201710.0027.v1

Ref. [35] studied the improvement of the solar flux intercepted by the receiver to increase the peak flux. They propose a new receiver, named Variable Velocity Receiver (VVR), Figure 2, consisting of a Traditional External Tubular Receiver (TETR) equipped with valves permitting the division of each panel in two independent panels. This increases the velocity of the heat transfer fluid in specific zones of the receiver avoiding tube overheating. The novel design also permits better aiming strategies, for an improved optical efficiency of the solar field and a possible reduction of the number of heliostats.

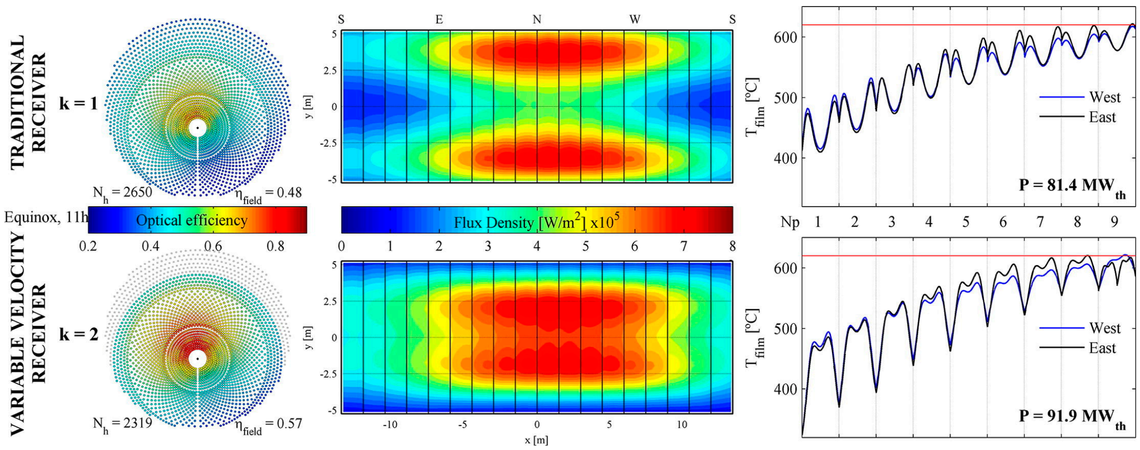

Figure 2 – Operation of the novel Variable Velocity Receiver proposed in [35] vs. a Traditional External Tubular Receiver. Reprinted from Applied Thermal Engineering, Vol. 128, M.R. Rodríguez-Sánchez, A. Sánchez-González, D. Santana, Feasibility study of a new concept of solar external receiver: Variable velocity receiver, Pages No. 335-344, Copyright (2018), with permission from Elsevier.

The size of the solar field required by a VVR is 12.5% smaller than the size required by a traditional TETR. Additionally, the VVR has benefit for the winter operation when the panels can be split in two, increasing the number of passes and the velocity of the heat transfer fluid.

High temperatures, thermal shocks and temperature gradient from a high, non-homogeneous and variable flux on the receiver walls are responsible for significant stresses. These stresses reduce the life-span of the receiver. Ref. [36] proposes an open loop approach to control the flux density distribution delivered on a CSP ST flat plate receiver. Various distributions of aiming points on the aperture of the receiver are considered. The approach provides interesting indications for the control of the heliostats that may drastically improve the life-span of the component.

Ref. [37] considers the optimization of a solar field layout with heliostats of different size. Although the use of a single heliostat size is openly questioned in the literature, there are no tools to design fields with heliostats of different sizes in the market. The paper addresses the problem of optimizing the heliostat field layout with two heliostats' sizes.

Ref. [38] numerically studied the influence of wind and return air on a volumetric receiver. Figure 3 presents a sketch of the receiver. The volumetric receiver is a highly porous material which absorbs solar radiation at different depth through its thickness. The effective area for solar absorption is larger than that of thermal radiation losses. A fan draws air through the absorbent pores, and the convective flow captures the heat absorbed. Thanks to the volumetric effect [39], the absorber thermal radiation loss is reduced.

Preprints (www.preprints.org) | NOT PEER-REVIEWED | Posted: 4 October 2017 doi:10.20944/preprints201710.0027.v1

Ref. [40] optically simulated the solar light radiation transmission from the heliostat field to a pressurized volumetric receiver. The optical efficiency of the heliostats' field and the local heat flux distribution within the SiC absorber is computed as a function of time and date, heliostats tracking error and receiver mounting height. The heat flux distribution within the absorber is non-uniform. The maximum heat flux density at the top area is up to $2.58 \cdot 10^9$ W/m^3. The pattern of field efficiency and maximum heat flux density of the absorber resembles those of the solar altitude angle during a day/year. The annual mean field efficiency and the maximum heat flux of the absorber decrease as the tracking error increases. As the receiver mounting height increases, both these parameters are marginally increasing.

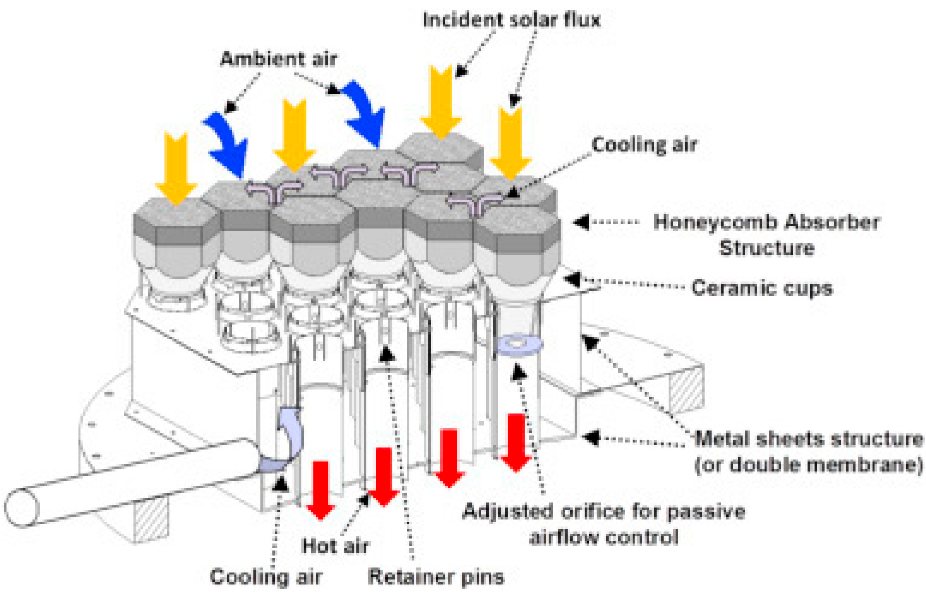

Figure 3 – Volumetric receiver used in [38]. Reprinted from Energy, Vol. 94, Roldán, M.I., Fernández-Reche, J. and Ballestrín, J., Computational fluid dynamics evaluation of the operating conditions for a volumetric receiver installed in a solar tower, Pages No. 844-856, Copyright (2016), with permission from Elsevier.

Ref. [41] proposed a dual-receiver with a surrounding solar field. The design couples an external boiling receiver and a cavity superheating receiver. The design provides a simple yet controllable heat flux distribution on both sections. The dual-receiver may produce superheated steam of 515 °C and 10.7 MPa with a solar heat absorbing efficiency of 86.55%. The efficiency improvement vs. two-external cylindrical receivers is 3.2%.

doi:10.20944/preprints201710.0027.v1

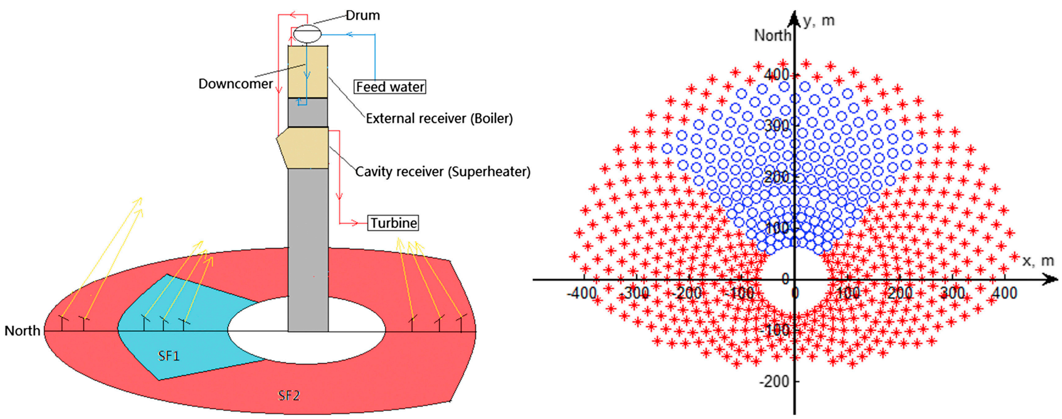

Figure 4 - Schematic diagram of the tower and heliostat field for the dual-receiver proposed in [41]. Reprinted from Applied Thermal Engineering, Vol. 91, Luo, Y., Du, X. and Wen, D., Novel design of central dual-receiver for solar power tower, Pages No. 1071-1081, Copyright (2015), with permission from Elsevier.

Ref. [42] optically modelled a Multi-Tube Cavity Receiver (MTCR). The solar flux exhibits a significant non-uniformity, showing a maximum flux of $5.141 \cdot 10^5$ W/m^2 on the tubes. When considering the random effect on the solar flux distribution, it is a good practice to treat the tracking errors as the random errors of the tracking angles. Multi-point aiming strategy of tracking helps to homogenize the flux and reduce the energy mal-distribution among the tubes. The tubes absorb 65.9% of the energy. The optical loss can be reduced significantly by the cavity effect, especially when the coating absorptivity is relatively low.

Heliostats account for about 50% of the capital cost of CSP ST plants. In conventional heliostats with vertical pedestals and azimuth-elevation drives, the support structure contributes 40–50% of this cost due to heavy cantilever arms required by the large spanning structures. Additional costs are imposed by expensive, difficult to maintain, drive mechanisms. Ref. [43] shows that a tripod heliostat substantially addresses these shortcomings for heliostats with aperture areas of 62 to 100 m^2. Ray-tracing simulations are included to estimate the performance penalties due to deformation under gravity and wind loads. The additional energy collection by a less-stiff, larger heliostat more than offsets the waste due to the greater deformation. The economics of CSP ST plants are strongly dependent on the cost of the heliostats rather than their optical performance. The cost of a tripod heliostat is reduced to \$72/m^2 which is less than half that of the conventional systems.

Ref. [44] studied the thermal performance of a cavity receiver in a CSP ST plant that relies on the spatial relationship of its polyhedral geometric inner surfaces. Based on model results, the thermal efficiency of the cavity receiver is shown to increase with the increase of incident heat flux. When the width-depth ratio decreased, the cavity efficiency increased first and then decreased. The total heat loss of the receiver varied differently with the increase of the heat absorption area to the aperture area ratio.

Ref. [45] modelled the thermal efficiency of multi-cavity CSP ST receivers. There is an optimal aperture flux that maximizes the local efficiency. This optimum is constrained by the maximum receiver working temperature. For this aperture flux, the thermal efficiency, receiver temperature, and RF temperature are calculated for an optimized flux distribution. In the proposed case study, it was found that a RF with a minimum convection coefficient between 250 and 500 W/m^2/K, permits to achieve a receiver thermal efficiency greater than 90%.

Preprints (www.preprints.org) | NOT PEER-REVIEWED | Posted: 4 October 2017 doi:10.20944/preprints201710.0027.v1

Ref. [46] investigated an array of high temperature pressurized air based solar receivers for Brayton, recuperated, and combined Brayton-Rankine cycles. The cluster of 500 solar receiver modules, attached to a hexagon-shaped secondary concentrator and arranged side-by-side in a honeycomb-type structure following a spherical fly-eye optical configuration, yield a peak solar energy to electricity efficiency of 37%.

Ref. [47] studied beam-down concentrating solar tower (BCST). BCST are known for easy installation and maintenance as well as lower convection heat loss of the central receiver. A point-line-coupling-focus BCST system using linear Fresnel heliostat as the first stage concentrator (heliostat) and hyperboloid/ellipsoid reflector as the tower reflector is proposed. Theoretical investigation on the ray concentrating mechanism with two commonly used reflector structures, namely, hyperboloid and ellipsoid, indicate that the ellipsoid system is superior in terms of interception efficiency over the hyperboloid system due to smaller astigmatism at the central receiver aperture, especially at larger facet tracking error [47]. The ellipsoid reflector shows significantly lower tower reflector shading efficiency. This is the result of the larger tower reflector surface area compared to that of the hyperboloid reflector. The total optical efficiency of the hyperboloid system is always better than that of the ellipsoid system. This efficiency gap decreases as the ratio increases. The hyperboloid tower reflector is claimed to be more promising and practical for the system investigated.

Ref. [48] studied volumetric air receivers. This component consists of a high temperature resistant cellular material which absorbs radiation and transfers the heat to an air flow which is fed from the ambient and from recirculated air. It is called volumetric, because the radiation may penetrate the "volume" of the receiver through the open, permeable cells of the material. In this way, a larger amount of heat transfer surface supports the solid to gaseous heat transfer in comparison to a tubular closed receiver. The heated air is directed to the steam generator of a conventional steam turbine system. Ref. [48] uses an advanced cellular metal honeycomb structure. It consists of winded pairs of flat and corrugated metal foils. Several variations of the pure linear honeycomb structure have been introduced to increase local turbulence and radial flow.

While some of these technologies may be easily implemented in future installations, those more sophisticated and innovative certainly require further studies.

3.5 Receiver coating

New materials and manufacturing processes are urgently needed to reduce costs and improve life-span of current designs. New materials are also needed for operation of components with higher temperatures and with reduced heat losses to also improve efficiency. While there is an abundant literature about new design of cycles, solar fields and receivers, thermal energy storage system, and receiver and power block fluids, manufacturing processes and new materials are only marginally covered in the literature despite their huge impacts on the costs of the CSP ST plants. Manufacturing of solar plant components is almost ignored.

Materials studies are mostly focused on the coating of the receiver. Solar receivers are presently mostly coated with a high sunlight absorptivity layer applied over the bare surface of the absorber receiver's tubes. Pyromark 2500 is the present standard coating. The coating enhances absorptivity and light-to-heat conversion. Ref. [49] studied the effect of the optical properties absorptivity and emissivity of these coatings on the thermal performance of a MS external receiver. Solar selective and non-selective coatings were analyzed and compared against the standard coating. The thermal efficiency increases up to 4% with the absorptivity of the coating. The emissivity has a very minor effect on the thermal performance of the receiver at its nominal working temperature. The efficiency only increases 0.6% when the emissivity of the coating decreases from 0.9 to 0.5. Improving the absorptivity of a non-selective coating leads to higher thermal efficiency than using a selective coating for current MS temperatures. For superheated steam cavity receivers, the effect of using a selective coating is noticeable at temperatures greater than 500 °C.

Ref. [50] also studied solar absorber coatings. The LCOE metric is used to attribute value to any high-temperature absorber coating. The LCOE gain efficiency is demonstrated on three different solar absorber coatings: Pyromark 2500, lanthanum strontium manganite oxide (LSM), and cobalt oxide (Co_3O_4). These coatings were used in a 100 MWe central tower receiver. Depending on the coating properties, an optimal reapplication interval was found that maximizes the LCOE gain efficiency. Pyromark 2500 paint enables a higher LCOE gain efficiency (0.182) than both LSM (0.139) and Co_3O_4 (0.083). The solar absorptance is by far the most influential parameter. The cost-effectiveness of Pyromark can be outperformed by a coating that would have a high initial solar absorptance (>0.95), a low initial degradation rate ($<2 \cdot 10^{-6}$ cycle^{-1}), and a low cost (<$500k per application).

Ref. [51] studied a novel MoSi2–Si3N4 hybrid composite, Figure 5. The MoSi2–Si3N4 absorber deposited onto Inconel substrate and capped with a Si3N4/Al2O3 layer on top is a promising selective coating for receivers operating in air at temperatures about 600 °C. Stacks with the Inconel/MoSi2-Si3N4/Si3N4/ Al2O3 structure on Inconel substrate show indeed good thermal stability in air.

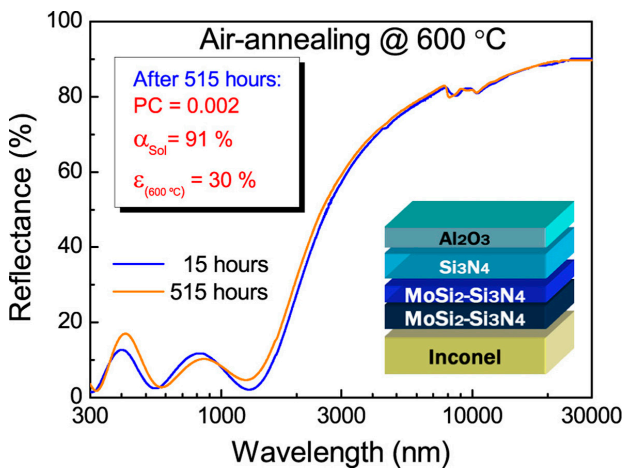

Figure 5 – Reflectance of new coating from Ref. [51]. Reprinted from Solar Energy Materials and Solar Cells, Vol. 174, Rodríguez-Palomo, A., Céspedes, E., Hernández-Pinilla, D. and Prieto, C., High-temperature air-stable solar selective coating based on MoSi 2–Si 3 N 4 composite, Pages No. 50-55, Copyright (2018), with permission from Elsevier.

3.6 Integrated solar combined cycle systems

While the use of NG in a boiler that supplement the solar field in the production of steam is common practice but it is not the best one as NG could be better used at double the thermal efficiency in a CCGT plant, it is otherwise an interesting opportunity to consider the coupling of a CSP ST plant with a CCGT plant.

Preprints (www.preprints.org) | NOT PEER-REVIEWED | Posted: 4 October 2017 doi:10.20944/preprints201710.0027.v1

Integrated solar combined cycle systems (ISCCS) are reviewed in Ref. [52]. ISCCS consist of three major components, CCGT, ST steam generator and solar field. The study indicates that very limited research has been directed so far toward the development of ISCCS with ST. Most of the ISCCS plants in operation today employ the PT technology. No known commercial ST ISCCS plant is operational in 2015. The study of ISCCS with ST is therefore an area of potential improvements still unexplored.

Ref. [53] modelled CSP PT vs. CSP ST coupled to a CCGT. The solar Rankine cycle is a single reheat regenerative Rankine cycle. The CCGT plant features a commercial gas turbine, with a dual pressure heat recovery steam generator. MS is the fluid to transfer heat to the water/steam of the solar Rankine cycle. Synthetic oil is used in the CCGT plant. The CSP ST has a higher collection efficiency than the CSP PT. The combined cycle is more efficient than the solar Rankine cycle. The CCGT plant coupled with a CSP ST is found to deliver the highest annual solar-to-electric efficiency of 21.8%.

As the integration of renewables with conventional power sources is presently discouraged, it is not expected that power plant burning fossil fuels will be integrated with solar fields, even if this is by far the best opportunity to convert solar thermal energy in electricity.

3.7 Integration with multi-effect distillation

As power and water supply are the two major issues humanity will face during this century, a robust growth of CSP around the world may be integrated with desalination for the next renewable energy breakthrough [54].

In desalination, seawater is separated into a low concentration of salts freshwater stream and a high concentration of salts brine. The most relevant desalination technologies are thermal desalination and membrane desalination. Thermal desalination utilizes heat, often by steam, to change phase of the seawater from liquid to vapor. Membrane desalination utilizes pressure, and hence electricity driven pumps, to force water through a semi-permeable membrane. In general, membrane desalination has advantages in terms of energy requirements and it is preferred where salinity is not very high. Seawater reverse osmosis (SWRO) membrane processes require less energy than multi-effect distillation (MED) thermal processes. However, Ref. [55] suggests that, for several locations, for example the Arabian Gulf, CSP plus MED may require 4% to 11% less input energy than CSP plus SWRO. This introduces an interesting opportunity for selected locations where MED may be competitive with SWRO. While SWRO does not need any integration of the desalination plant with the CSP plant, as the electricity needed can be produced everywhere, MED may be easily and conveniently integrated with a CSP saving the condenser costs.

MED produces high quality water from sea or brackish water. Concentration of total dissolved solids (TDS) is 25 mg/l or less. MED units range from about 100 m^3/day up to 36,400 m^3/day. While single units may be utilized in smaller volume applications, multiple units may be combined to further increase capacity [54].

In desert installations, far from the coast, the condenser is air cooled, and this limits the expansion of steam in turbine. While in coastal locations the condenser may certainly be, water cooled for better performances of the plant, alternatively, the condenser may also be replaced by a MED thermal desalination module. The steam generated is superheated to 380 °C to 580 °C and the steam temperature for the MED is not higher than 135 °C [54]. Hence, the steam has sufficient energy to produce electricity before entering the MED. If power is the main product, a water condenser may work better. However, where water is more precious than power, and MED is competitive with SWRO, integration of CSP ST with MED is a local renewable energy break-through.

Ref. [56] proposed solar thermal sea water desalination, however adopting multi-stage flash evaporation (MSF) rather than MED. The theoretical study considers a ST with a volumetric solar receiver, a power cycle water/steam Rankine, MS as the receiver fluid, MS TES plus the MSF. The seawater is heated by the saturated steam-water mixture coming from the steam turbine. This eliminates the condenser. Considering the advantages MED has vs. MSF [54], presently the primary thermal desalination option, the advantages mentioned in [56] will be further strengthen when using MED.

3.8 Regionalization

Places with lot of sun to make plausible CSP ST plant may have very different climate conditions. Proximity to coast, availability of land, orography of land, coupling to desalination, availability of natural gas, prevailing weather conditions, sand storms, wind load, rainfall, all play a key role to reshape one single design to match local conditions. Despite some design concepts may certainly be shared between many different CSP installations, regionalization plays a significant role in providing the sought outcomes in terms of performance, cost and life span of a plant.

Ref. [14] studies the technical, financial and policy drivers and barriers for adopting CSP ST technologies in India. Especially CSP ST with external cylindrical or cavity receivers with storage look promising. This technology is particularly relevant to the Jawaharlal Nehru National Solar Mission (JNNSM) aimed at achieving grid-connected solar power of 1800 MW by 2022.

Ref. [57] reviews the CSP plants installed in India and discusses the growth of the electricity generated by CSP in India, with targets grown to 100,000 MW by 2022.

Ref. [58] report on the design and construction of a CSP ST demonstration plant in Saudi Arabia, an area of extreme solar intensity and temperatures. The solar receiver was made of alloy steel. Ten heliostats were chosen, featuring two motors were used to control the heliostat rotational and elevation movements. The thermal fluid was a MS mixture 60% $NaNO_3$ and 40% KNO_3. Cold and hot storage tanks were manufactured from steel insulated with calcium silicate from all sides. A one-meter high and one and a half-meter diameter cylindrical vessel was adopted for each of the cold and hot tanks. The design thermal power was 13 kW. The thermal power released by the MS was 12.31 kW. The thermal power transferred to the water/steam was 11.26 kW. The work proves the value of small demonstration plants. Small demonstration plant is needed for regionalization in every location where conditions may differ considerably from the areas of well-established designs to perform a proper regionalization of the design.

The energy and exergy analyses of sCO_2 recompression Brayton cycles of Ref. [32] is performed for different locations in Saudi Arabia. The exercise returns a ranking by location based on the selected CSP ST configuration.

Ref. [59] simulated the behavior of the Spanish GEMASOLAR plant under different climates. The analysis is performed for different locations of mainland China. An estimation of both annual energy production and return of the investment was provided. Simulations were made with and without hybridization with combustion of fossil fuels and with same or modified nominal power. Annual overall efficiencies were about 14% for the 20 MW power plant (GEMASOLAR nominal power). Down-scaled plants were able of maintaining an efficiency of 14.97% for a 10 MW power plant.

 doi:10.20944/preprints201710.0027.v1

Ref. [60] compares under the Algerian climate a Rankine cycle with a tubular water/steam receiver and a Brayton cycle with volumetric air receiver. The tubular receiver Rankine cycle is economically slightly disadvantaged vs. the volumetric air receiver Brayton cycle, but it works better especially under lower solar radiation intensity. The GT requires higher operating temperatures which are usually difficult to reach throughout the year.

4. Conclusions

The current trends in the development of concentrated solar power (CSP) solar tower (ST) installations have been reviewed. Improvements are being sought for efficiency of plant, installation cost, life-span and operation cost. Materials and manufacturing processes, design of solar field and receiver, including fluids, cycle and materials, optimal management of daily and seasonal operation of the plant, new thermal energy storage concepts, integration of solar plant with thermal desalination, integration of solar plant with combined cycle gas turbine (CCGT) installations and finally, specialization and regionalization of the project specification, are the key areas of progress of CSP ST technology.

While it is expected that CSP ST installations will grow considerably in the next few years, there is not yet a better solution all-inclusive than the use of molten salt (MS) as receiver fluid (RF) and thermal energy storage (TES) fluid, with classic solar field heliostats and receivers, driving a water/steam superheated Rankine cycle steam cycle.

The different alternatives that are presently under study at different stages of development may only progress slowly, benefiting from real world experiences requiring time rather than simulations or laboratory experiments.

Cost of plants are not expected to reduce drastically, even if convergence on few selected designs of heliostats and receivers could be beneficial to their improvement and cost reduction, with manufacturing of components in large scale and significant feed-backs from real world operation expected to be a major driver of the developments.

Acknowledgments: The authors received no funding.

Conflicts of Interest: The authors declare no conflict of interest.

Authors' contributions: The authors equally contributed to the review of the papers and the writing of the manuscript.

Symbols

η	efficiency
ε	capacity factor
E	electric energy
P	electric power
Q	thermal energy
sCO_2	supercritical carbon dioxide

Acronyms

BCST	beam-down concentrating solar tower
CSP	concentrated solar power
CCGT	combined cycle gas turbine

 doi:10.20944/preprints201710.0027.v1

GT	gas turbine
ISCCS	Integrated solar combined cycle system
ISEGS	Ivanpah Solar Electric Generating System
LCOE	Levelized Cost of Electricity
MED	multi effect distillation
MS	molten salt
MTCR	Multi Tube Cavity Receiver
NG	natural gas
PT	Parabolic Trough
PV	photovoltaic
RF	receiver fluid
RMCI	Recompression with Main Compression Intercooling
SEGS	Solar Energy Generating Systems
ST	Solar Tower
SWRO	sea water reverse osmosis
TCES	thermochemical energy storage
TES	thermal energy storage
TETR	Traditional External Tubular Receiver
VVR	Variable Velocity Receiver

References

[1] Romero-Alvarez, M. and Zarza, E., Concentrating solar thermal power. Handbook of energy efficiency and renewable energy, 2007:21-1.

[2] del Río, P., Peñasco, C. and Mir-Artigues, P., An overview of drivers and barriers to concentrated solar power in the European Union. Renewable and Sustainable Energy Reviews, 2018, 81, pp.1019-1029.

[3] de Souza, L.E.V. and Cavalcante, A.M.G., Concentrated Solar Power deployment in emerging economies: The cases of China and Brazil. Renewable and Sustainable Energy Reviews, 2017, 72, pp.1094-1103.

[4] Margolis, R., Coggeshall, C. and Zuboy, J., SunShot vision study. US Dept. of Energy, 2012.

[5] Kearney, D. and Herrmann, U., Engineering evaluation of a molten salt heat transfer fluid in a parabolic trough solar field. National Renewal Energy Laboratoy, 2006.

[6] Feldhoff, J.F., Schmitz, K., Eck, M., Schnatbaum-Laumann, L., Laing, D., Ortiz-Vives, F. and Schulte-Fischedick, J., Comparative system analysis of direct steam generation and synthetic oil parabolic trough power plants with integrated thermal storage. Solar Energy, 2012, 86(1): 520-530.

[7] Bendt, P., Rabl, A., Gaul, H.W. and Reed, K.A., Optical analysis and optimization of line focus solar collectors (No. NREL/TR-34-92). National Renewable Energy Laboratory (NREL), Golden, CO, 1979.

[8] Boretti, A., Concentrated Solar Power Plants Capacity Factors: A Review, Nonlinear Approaches in Engineering Applications Energy: Vibrations, and Modern Applications, Liming Dai, Eds., Reza N. Jazar, Springer, New York, 2017.

[9] Reilly, H.E. and Kolb, G.J., An evaluation of molten-salt power towers including results of the solar two project (No. SAND2001-3674). Sandia National Labs., Albuquerque, NM (US); Sandia National Labs., Livermore, CA (US), 2007.

[10] Radosevich, L.G., Final Report on the Power Production Phase of the 10 MWe Solar Thermal Central Receiver Pilot Plant, SAND87-8022. Sandia National Laboratories, Albuquerque, NM, 1988.

[11] Thermoflow, Inc., "Thermoflow". www.thermoflow.com/, Retrieved August 28, 2017.

[12] National renewable Energy Laboratory, Concentrating Solar Power Projects by Project Name. www.nrel.gov/csp/solarpaces/by_project.cfm , Retrieved August 28, 2017.
[13] Energy Information Administration. Electricity data browser – Plant Level Data. www.eia.gov/electricity/data/browser/ , Retrieved August 28, 2017.
[14] Srilakshmi, G., Venkatesh, V., Thirumalai, N.C. and Suresh, N.S., Challenges and opportunities for Solar Tower technology in India. Renewable and Sustainable Energy Reviews, 2015, 45:698-709.
[15] Hoffschmidt, B., Receivers for Solar Tower Systems. CNRS 2014 SFERA School, June 25-27, 2014, Font Romeu, France. http://elib.dlr.de/94540/1/SFERA2014_SolarTowerReceivers_final.pdf, Retrieved August 28, 2017.
[16] Vignarooban, K., Xu, X., Arvay, A., Hsu, K. and Kannan, A.M., Heat transfer fluids for concentrating solar power systems–a review. Applied Energy, 2015, 146, pp.383-396.
[17] Liu, M., Belusko, M., Tay, N.S. and Bruno, F., Impact of the heat transfer fluid in a flat plate phase change thermal storage unit for concentrated solar tower plants. Solar Energy, 2014, 101:220-231.
[18] Pelay, U., Luo, L., Fan, Y., Stitou, D. and Rood, M., Thermal energy storage systems for concentrated solar power plants. Renewable and Sustainable Energy Reviews, 2017, 79:82-100.
[19] González-Roubaud, E., Pérez-Osorio, D. and Prieto, C., Review of commercial thermal energy storage in concentrated solar power plants: Steam vs. molten salts. Renewable and Sustainable Energy Reviews, 2017, 80:133-148.
[20] Zhang, H., Benoit, H., Perez-Lopèz, I., Flamant, G., Tan, T. and Baeyens, J., High-efficiency solar power towers using particle suspensions as heat carrier in the receiver and in the thermal energy storage. Renewable Energy. 2017.
[21] Alexopoulos, S. and Hoffschmidt, B., Advances in solar tower technology. Wiley Interdisciplinary Reviews: Energy and Environment, 2017, 6(1).
[22] Peng, X., Root, T.W. and Maravelias, C.T., Storing solar energy with chemistry: the role of thermochemical storage in concentrating solar power. Green Chemistry, 2017, 19(10):2427-2438.
[23] Tescari, S., Singh, A., Agrafiotis, C., de Oliveira, L., Breuer, S., Schlögl-Knothe, B., Roeb, M. and Sattler, C., Experimental evaluation of a pilot-scale thermochemical storage system for a concentrated solar power plant. Applied Energy, 2017, 189:66-75.
[24] Pacheco, J.E., Wolf, T. and Muley, N., Incorporating Supercritical Steam Turbines Into Advanced Molten-Salt Power Tower Plants: Feasibility and Performance. Sandia National Laboratories, Albuquerque, NM, Report No. SAN2013-1960, 2013.
[25] Turchi, C.S., Ma, Z., Neises, T.W. and Wagner, M.J., Thermodynamic study of advanced supercritical carbon dioxide power cycles for concentrating solar power systems. Journal of Solar Energy Engineering, 2013, 135(4):041007.
[26] Zheng, H., Yu, X., Su, Y., Riffat, S. and Xiong, J., Thermodynamic analysis of an idealised solar tower thermal power plant. Applied Thermal Engineering, 2015, 81:271-278.
[27] Schmitt, J., Wilkes, J., Allison, T., Bennett, J., Wygant, K. and Pelton, R., Lowering the Levelized Cost of Electricity of a Concentrating Solar Power Tower with a Supercritical Carbon Dioxide Power Cycle. In ASME Turbo Expo 2017: Turbomachinery Technical Conference and Exposition (pp. V009T38A028-V009T38A028). American Society of Mechanical Engineers, 2017, June.
[28] Stein, W.H. and Buck, R., Advanced power cycles for concentrated solar power. Solar Energy, 2017, 152:91-105.

[29] Binotti, M., Astolfi, M., Campanari, S., Manzolini, G. and Silva, P., Preliminary assessment of sCO 2 cycles for power generation in CSP solar tower plants. Applied Energy.
[30] Wang, K., He, Y.L. and Zhu, H.H., Integration between supercritical CO 2 Brayton cycles and molten salt solar power towers: A review and a comprehensive comparison of different cycle layouts. Applied Energy, 2017, 195:819-836.
[31] Rodríguez-Sánchez, M.R., Sánchez-González, A., González-Gómez, P.A., Marugán-Cruz, C. and Santana, D., Thermodynamic and economic assessment of a new generation of subcritical and supercritical solar power towers. Energy, 2017, 118:534-544.
[32] Atif, M. and Al-Sulaiman, F.A., Energy and exergy analyses of solar tower power plant driven supercritical carbon dioxide recompression cycles for six different locations. Renewable and Sustainable Energy Reviews, 2017, 68:153-167.
[33] Poživil, P. and Steinfeld, A., Integration of a Pressurized-Air Solar Receiver Array to a Gas Turbine Power Cycle for Solar Tower Applications. Journal of Solar Energy Engineering, 2017, 139(4), p.041007.
[34] Ho, C.K. and Iverson, B.D., Review of high-temperature central receiver designs for concentrating solar power. Renewable and Sustainable Energy Reviews, 2014, 29, pp.835-846.
[35] Rodríguez-Sánchez, M.R., Sánchez-González, A. and Santana, D., Feasibility study of a new concept of solar external receiver: variable velocity receiver. Applied Thermal Engineering. 2018. 128, pp. 335-344.
[36] Salomé, A., Chhel, F., Flamant, G., Ferrière, A. and Thiery, F., Control of the flux distribution on a solar tower receiver using an optimized aiming point strategy: Application to THEMIS solar tower. Solar Energy, 2013, 94:352-366.
[37] Carrizosa, E., Domínguez-Bravo, C.A., Fernández-Cara, E. and Quero, M., An optimization tool to design the field of a solar power tower plant allowing heliostats of different sizes. International Journal of Energy Research. 2017.
[38] Roldán, M.I., Fernández-Reche, J. and Ballestrín, J., Computational fluid dynamics evaluation of the operating conditions for a volumetric receiver installed in a solar tower. Energy, 2016, 94, pp.844-856.
[39] Hoffschmidt, B., Tellez, F.M., Valverde, A., Fernández, J. and Fernández, V., Performance evaluation of the 200-kWth HiTRec-II open volumetric air receiver, 2003. Journal of Solar Energy Engineering, 125(1), pp.87-94.
[40] He, Y.L., Cui, F.Q., Cheng, Z.D., Li, Z.Y. and Tao, W.Q., Numerical simulation of solar radiation transmission process for the solar tower power plant: from the heliostat field to the pressurized volumetric receiver. Applied Thermal Engineering, 2013, 61(2):583-595.
[41] Luo, Y., Du, X. and Wen, D., Novel design of central dual-receiver for solar power tower. Applied Thermal Engineering, 2015, 91, pp.1071-1081.
[42] Qiu, Y., He, Y.L., Li, P. and Du, B.C., A comprehensive model for analysis of real-time optical performance of a solar power tower with a multi-tube cavity receiver. Applied Energy, 2017, 185:589-603.
[43] Thalange, V.C., Dalvi, V.H., Mahajani, S.M., Panse, S.V., Joshi, J.B. and Patil, R.N., Design, optimization and optical performance study of tripod heliostat for solar power tower plant. Energy, 2017, 135:610-624.
[44] Deng, Q., Xiao, X., Hao, Y., Wang, Q., Hu, T. and Wang, Y., Heat transfer performance evaluation of a large-size cavity receiver in the solar power tower plant based on angle factors. Solar Energy, 2017, 148:78-86.
[45] Fleming, A., Folsom, C., Ban, H. and Ma, Z., 2017. A general method to analyze the thermal performance of multi-cavity concentrating solar power receivers. Solar Energy, 2017, 150:608-618.

Preprints (www.preprints.org) | NOT PEER-REVIEWED | Posted: 4 October 2017 doi:10.20944/preprints201710.0027.v1

[46] Hischier, I., Poživil, P. and Steinfeld, A., Optical and Thermal Analysis of a Pressurized-Air Receiver Cluster for a 50 MWe Solar Power Tower. Journal of Solar Energy Engineering, 2015, 137(6), p.061002.

[47] Li, X., Lin, M., Dai, Y. and Wang, C.H., Comparison-based optical assessment of hyperboloid and ellipsoid reflectors in a beam-down solar tower system with linear Fresnel heliostats. Journal of Solar Energy Engineering, 2017, 139(6), p.061003.

[48] Pabst, C., Feckler, G., Schmitz, S., Smirnova, O., Capuano, R., Hirth, P. and Fend, T., Experimental performance of an advanced metal volumetric air receiver for Solar Towers. Renewable Energy, 2017, 106, pp.91-98.

[49] López-Herraiz, M., Fernández, A.B., Martinez, N. and Gallas, M., Effect of the optical properties of the coating of a concentrated solar power central receiver on its thermal efficiency. Solar Energy Materials and Solar Cells, 2017, 159:66-72.

[50] Boubault, A., Ho, C.K., Hall, A., Lambert, T.N. and Ambrosini, A., Durability of solar absorber coatings and their cost-effectiveness. Solar Energy Materials and Solar Cells, 2017, 166, pp.176-184.

[51] Rodríguez-Palomo, A., Céspedes, E., Hernández-Pinilla, D. and Prieto, C., High-temperature air-stable solar selective coating based on MoSi 2–Si 3 N 4 composite. Solar Energy Materials and Solar Cells, 2018, 174, pp.50-55.

[52] Okoroigwe, E. and Madhlopa, A., An integrated combined cycle system driven by a solar tower: A review. Renewable and Sustainable Energy Reviews, 2016, 57:337-350.

[53] Franchini, G., Perdichizzi, A., Ravelli, S. and Barigozzi, G., A comparative study between parabolic trough and solar tower technologies in Solar Rankine Cycle and Integrated Solar Combined Cycle plants. Solar Energy, 2013, 98:302-314.

[54] Zachary, J. and Layman, C.M., 2010. Adding Desalination to Solar Hybrid and Fossil Plants. Power, 154(5).

[55] Trieb, F. and Müller-Steinhagen, H., 2008. Concentrating solar power for seawater desalination in the Middle East and North Africa. Desalination, 220(1-3):165-183.

[56] Demir, M.E. and Dincer, I., Development and analysis of a new integrated solar energy system with thermal storage for fresh water and power production. International Journal of Energy Research. 2017, DOI: 10.1002/er.3846.

[57] Kumar, A., Prakash, O. and Dube, A., A review on progress of concentrated solar power in India. Renewable and Sustainable Energy Reviews, 2017, 79:304-307.

[58] Abu-Hamdeh, N.H. and Alnefaie, K.A., Design considerations and construction of an experimental prototype of concentrating solar power tower system in Saudi Arabia. Energy Conversion and Management, 2016, 117:63-73.

[59] Amadei, C.A., Allesina, G., Tartarini, P. and Yuting, W., Simulation of GEMASOLAR-based solar tower plants for the Chinese energy market: Influence of plant downsizing and location change. Renewable energy, 2013, 55:366-373.

[60] Yamani, N., Khellaf, A., Mohammedi, K. and Behar, O., Assessment of solar thermal tower technology under Algerian climate. Energy, 2017, 126:444-460.